LABORATORI NAZIONALI DI FRASCATI

LNF-10/20(IR)
September 20, 2010

CMS TRAPEZOIDAL GEM FOILS STRUCTURAL ANALYSIS

G.Raffone
INFN, Laboratori Nazionali di Frascati, P.O. Box 13, I-00044 Frascati, Italy.

Abstract

The demand of large area GEM detectors requires extreme working conditions of the layered foils from structural point of view; larger area need higher biaxial tensile loads to overcome large deflections and the related stresses may exceed the copper yield limit just around the holes; the present work shows that for a trapezoidal CMS GEM foil (W=1040 mm; L1=530 mm; L2=345 mm) the sag due its own weight is about $f \cong 28.6$ μm (electrostatic loads not included) for a tensioning of S=1 N/mm; the related stresses are lower than the yield only in a biaxial load. Numerical results are from ANSYS Educational v.10 [1] and their level of accuracy is very good when compared to some theoretical and experimental results.

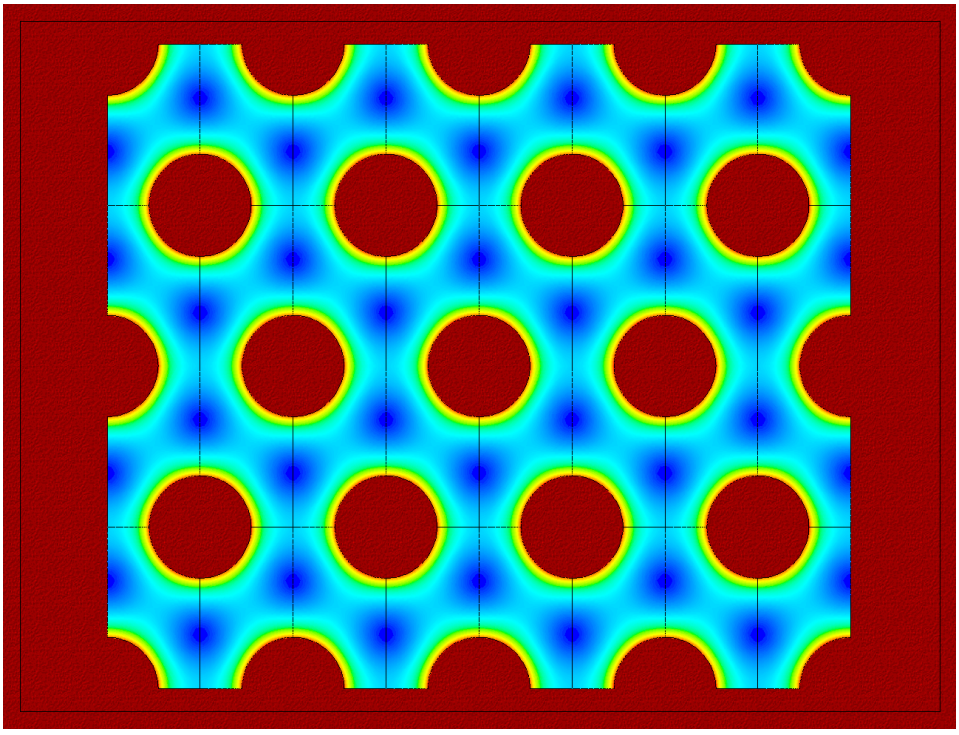

5 μm copper layer equivalent stresses (HMH) under a biaxial load showing the hexagonal symmetry.

1 - Plane stress homogenization.

The GEM tri-layered foils have hexagonal symmetry due to the holes pattern, i.e. they behave to the common in-plane isotropic thin plates; strictly speaking the GEM foils are *transversely isotropic* since the out-of-plane mechanical properties are different because of the layering [a].

1§1 - Local stresses of a perforated single layer foil in plane stress.

The in-plane isotropy of the GEM foils is a *macroscopic isotropy*, in the sense that remote tensile or bending loads give the same overall displacements field whatever direction of the applied loads is; this is not true at the level of the texture element, that is the local stresses and strains depend on the direction of the external loads; thus *the GEM foils are isotropic macroscopically but highly anisotropic at the level of the texture element* [2]; in other words the different behaviours of the stresses and strains of the texture element along two orthogonal directions under the same remote loadings are averaged by the overall hexagonal symmetry giving the same macroscopic displacements in those directions, i.e. in any direction. Fig. 1§1-1 shows displacements and stresses of the texture element (considering only the 5 μm Cu layer) subjected to an uniaxial tensile load along X equal to $\sigma_{uniform,\,Cu} = 86.5$ MPa ; as usual local severe stress concentrations around the holes are observed at $\pi/2$ and 0 (respectively $\sigma_x = +367$ MPa and $\sigma_y = -65.4$ MPa). That numerical result is not straightforward but it is obtained by a simple trial-and-error procedure [b]; Fig. 1§1-2 shows the same results when the same remote tensile load is applied along Y; the stresses at $\pi/2$ and 0 are $\sigma_x = -149$ MPa and $\sigma_y = +289$ MPa ; then *the same load applied along two orthogonal directions gives unequal local stress and strain fields*.

---

[a] Even if the effect of the transversal properties on membrane-type and bending-type problem is negligible for moderately thin composite plates, the assumption of the transversal isotropy is fundamental to get consistent and correct expressions of the averaged properties of any layered plate in plane stress. A simple but general and elegant method of averaging is due to Backus (see Appendix A) but it is limited to plane stress problems (such as the in-plane tensioning) and it not so accurate in bending-type problems (similar to the plane stress problems but the stress gradients through the thickness and out-of-plane shears); the basic averaging criteria of the bending-type problems are given in CLT (classical lamination theory).

[b] Given the remote tensile load $\sigma_{uniform,\,Cu} = 86.5$ MPa then symmetric trial displacements are applied on the X-normal boundaries leaving the others free to move in the Y direction (all displacements on boundaries are coupled also, of course); then the corresponding remote tensile load (the error) is given by the nodal forces balance on the same boundaries (the arrows denoted by NFOR); it must be underlined that the application of the tensile load $\sigma_{uniform,\,Cu} = 86.5$ MPa on the boundaries gives misleading results since along the same boundaries only the displacements are constant as the symmetry, but neither the stresses nor the strains.

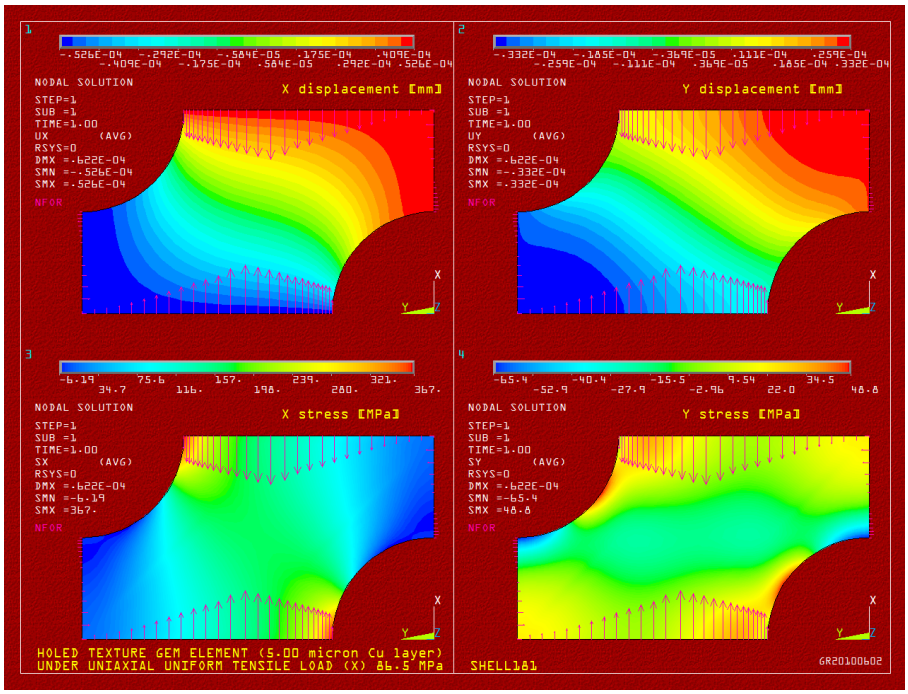

Fig. 1§1-1 Texture GEM element (5 µm Cu layer only) under $\sigma_{uniform,\,Cu} = 86.5$ MPa tensile load along X.

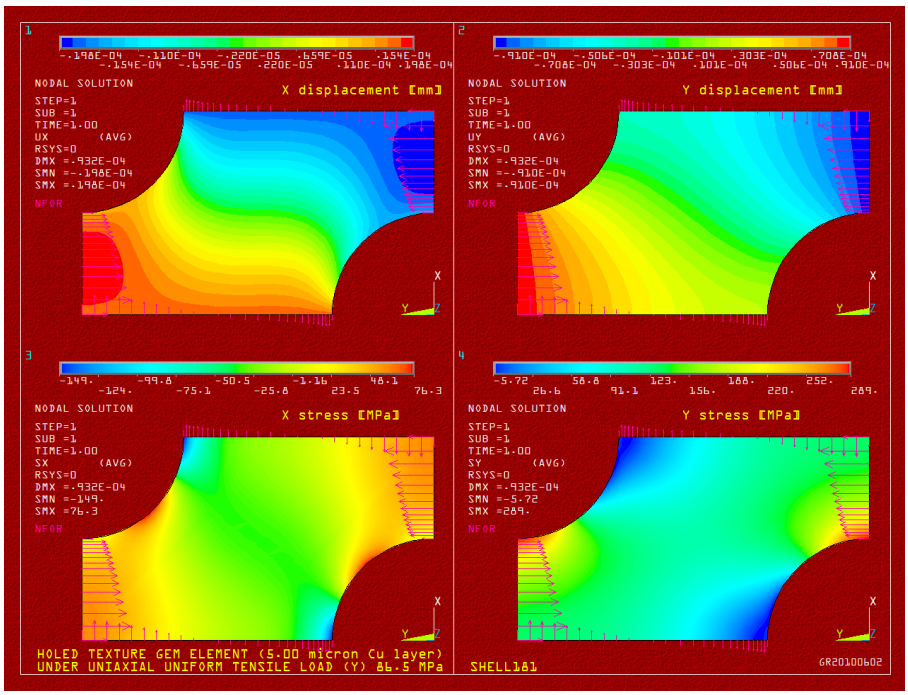

Fig. 1§1-2 Texture GEM element (5 µm Cu layer only) under $\sigma_{uniform,\,Cu} = 86.5$ MPa tensile load along Y.

It is not surprising that the ratio of the imposed displacements that give the same tensile load $\sigma_{uniform,Cu} = 86.5$ MPa in X and Y (respectively $U_x\big|_x = \pm 0.052565$ µm in Fig. 1§1-1 and $U_y\big|_y = \pm 0.091045$ µm in Fig. 1§1-2) is equal to $\sqrt{3}$, that is *the macroscopic strains* $\bar{\varepsilon}_x\big|_x = 4\big|U_x\big|_x\big|/p$ *and* $\bar{\varepsilon}_y\big|_y = 4\big|U_y\big|_y\big|/\sqrt{3}p$ *are equal (i.e.* $\bar{\varepsilon}_x\big|_x = \bar{\varepsilon}_y\big|_y$*) under the same uniaxial tensile load*, being $p = 140$ µm the *ligament length* [c].

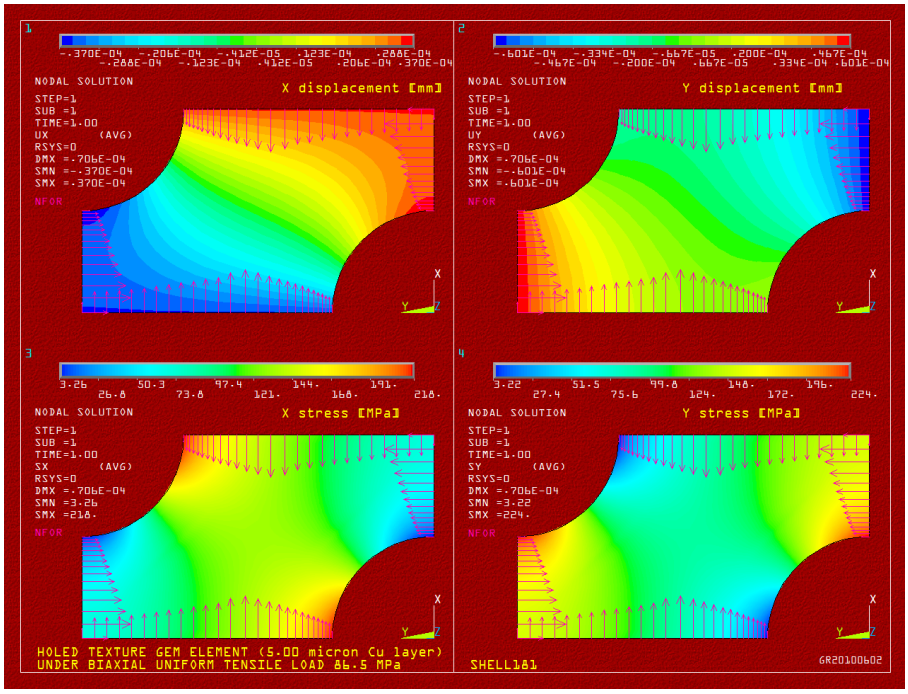

Fig. 1§1-3 Texture GEM element (5 µm Cu layer only) under $\sigma_{uniform,Cu} = 86.5$ MPa biaxial tensile load.

Fig. 1§1-3 shows the texture element under a biaxial load; once again $\bar{\varepsilon}_x\big|_{xy} = \bar{\varepsilon}_y\big|_{xy}$ since $U_x\big|_{xy} = \pm 0.034670$ µm [d] and $U_y\big|_{xy} = \pm 0.060050$ µm are the imposed displacements that give the biaxial remote stress $\sigma_{uniform,Cu} = 86.5$ MPa ; the local stresses at $\pi/2$ and

[c] That simulation can be considered and indirect demonstration of the *macroscopic isotropy* of the GEM foils.

[d] In Fig. 1§1-3 the maximum, minimum X-displacement $U_{x,\max,\min}\big|_{xy} = \pm 0.037070$ µm is located on the hole and the nodal averaged plot may be badly understood; the solution print out gives a displacement of $U_x\big|_{xy} = \pm 0.034670$ µm on all the X-normal boundaries; same considerations can be made on Fig. 1§1-1 ($U_y\big|_x = \pm 0.031002$ µm versus $U_{y,\max,\min}\big|_x = \pm 0.033226$ µm) and on Fig. 1§1-2. ($U_x\big|_y = \pm 0.017899$ µm versus $U_{x,\max,\min}\big|_y = \pm 0.019782$ µm).

0 are $\sigma_x = +218$ MPa and $\sigma_y = +224$ MPa (the difference is not due to numerical approximation or round-off); they are much lower than the previous ones, as expected [e].

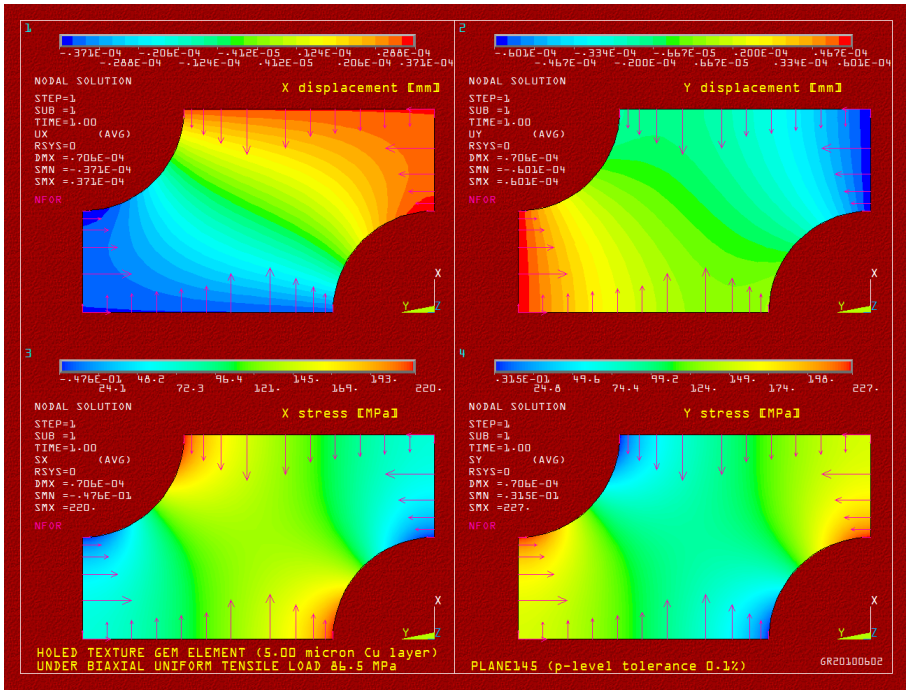

Fig. 1§1-4 Same as Fig. 1§1-3 but with p-method.

The stress concentration factors are easily computed for each configuration (the subscript is the load direction, the superscript the location): $K_x^{\pi/2} = 367/86.5 = 4.24$, $K_x^{0} = -65.4/86.5 = -0.76$, $K_y^{\pi/2} = -149/86.5 = -1.72$, $K_y^{0} = 289/86.5 = 3.34$, $K_{xy}^{\pi/2} = 218/86.5 = 2.52$, $K_{xy}^{0} = 224/86.5 = 2.59$ [f]; the more interesting factors are $K_x^{\pi/2}$, K_y^{0}, $K_{xy}^{\pi/2}$, K_{xy}^{0} that give the peak stresses; they do not depend on the material but only on the geometry, that is on the *solidity ratio* $0 \le d/p \le 1$ (being $d = 70$ µm the hole diameter) and on the angle (60° in GEM); these factors are always greater than

[e] The stress lowering due to the biaxial load is well known: in an uniaxial tensile load the maximum stress at $\pi/2$ is a tensile stress having the same direction of the load; then if another tensile load is applied along the perpendicular direction, that maximum stress is lowered since the region at $\pi/2$ is unloaded (and vice versa).

[f] Note that $Kxy^{\pi/2} = Kx^{\pi/2} + Ky^{\pi/2}$ and $Kxy^{0} = Kx^{0} + Ky^{0}$ due to the superposition principle.

those referred to a single hole in an infinite plate [3] ($K_x^{\pi/2} = K_y^{0} = 3$ and $K_{xy}^{\pi/2} = K_{xy}^{0} = 2$) because *the Saint Venant's principle cannot be applied* [g].

Furthermore all the stresses shown in the previous pictures are always underestimated (and the stress concentration factors too) because of the poorly mesh refinement in the high stress gradient regions; Fig. 1§1-4 shows the result for a biaxial load obtained by means of the high order accuracy p-method; the numerical improvements are not so significant between plane p-elements and shell h-elements that will be adopted in the bending-type problems (but the coarse mesh and the highly accurate polynomial interpolation).

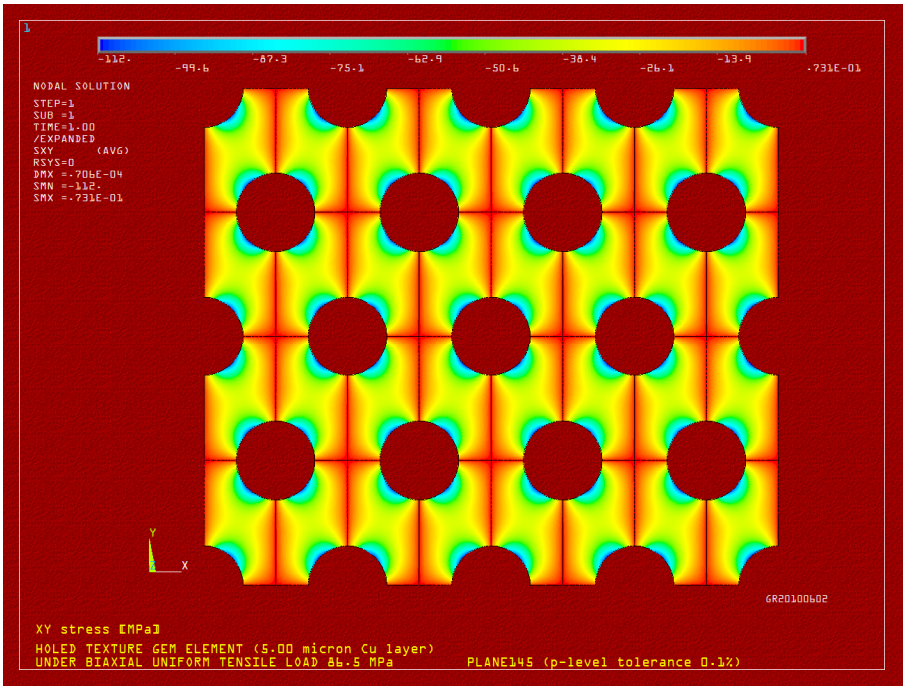

Fig. 1§1-5 Shear stresses of the 5 μm Cu layer under $\sigma_{uniform,\,Cu} = 86.5$ MPa biaxial tensile load.

Fig. 1§1-5 shows the shear stresses due to the biaxial load $\sigma_{uniform,\,Cu} = 86.5$ MPa ; the cover picture refers to the HMH equivalent stresses under the same biaxial load.

---

[g] The solidity ratio of the GEM foils is 1/2 and then there is a mutual influence between two neighbouring holes; the Saint Venant's principle holds in the limiting case $d/p \ll 1$ where the holes are isolated singularities, the concentration factors approach those of the infinite plate, the texture becomes locally isotropic.

Tab. 1§1-1 shows the stress concentration factors with p-method as illustrated in Fig. 1§1-6 to Fig. 1§1-8; they are a little bit greater than before.

	uniaxial X	uniaxial Y	biaxial XY
π/2	4.40 [4]	-1.85	2.55 [2]
0	-0.80	3.42 [2]	2.62 [4]

Tab. 1§1-1 Stress Concentration Factors (SCF) of GEM foils with p-method.

The factors $K_y^{\,0} = 3.42$ and $K_{xy}^{\,\pi/2} = 2.55$ agree with Horvay theoretical results [2] (see on the right of Fig. 1§1-9) but it seems that they are not the worst as the experimental data reported by O'Donnell [4] (Sampson photoelastic measurements, see on the left of Fig. 1§1-9); *the O'Donnell experimental factors agree very well with the values of* $K_x^{\,\pi/2} = 4.40$ *and* $K_{xy}^{\,0} = 2.62$ that must be considered in the design.

Due to the hexagonal symmetry the stress concentration factors for uniaxial loadings are the same every 60°, that is $K_x^{\,\pi/2} = 4.40$ and $K_x^{\,0} = -0.80$ are the stress multipliers if tensioning along 0°,60°,120° while $K_y^{\,0} = 3.42$ and $K_y^{\,\pi/2} = -1.85$ if tensioning along 30°,90°,150°; the biaxial factors $K_{xy}^{\,\pi/2} = 2.55$ and $K_{xy}^{\,0} = 2.62$ repeat every 30°.

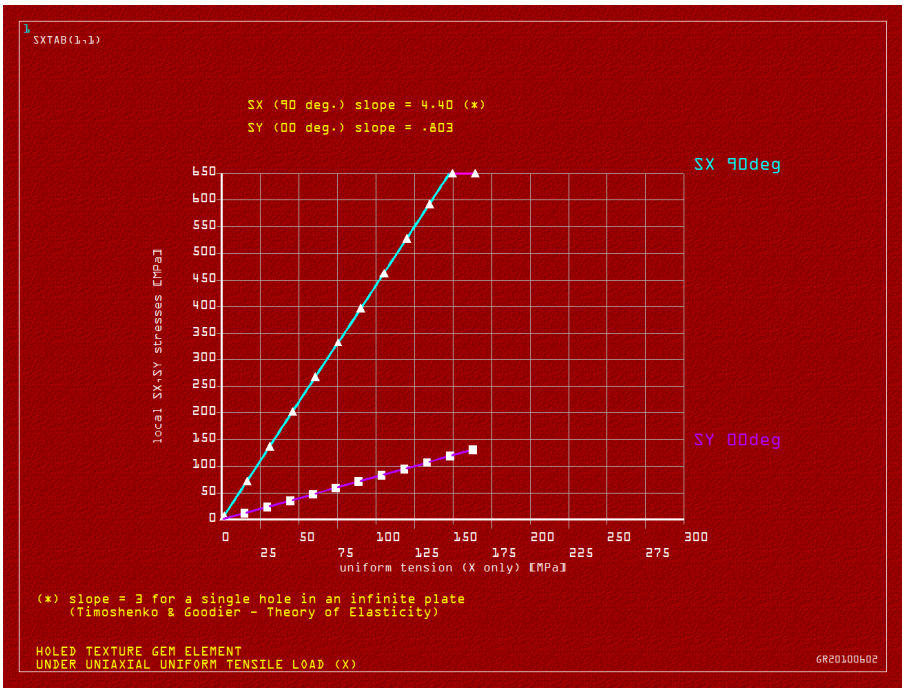

Fig. 1§1-6 Stress peaks varing the uniform tensile load along X.

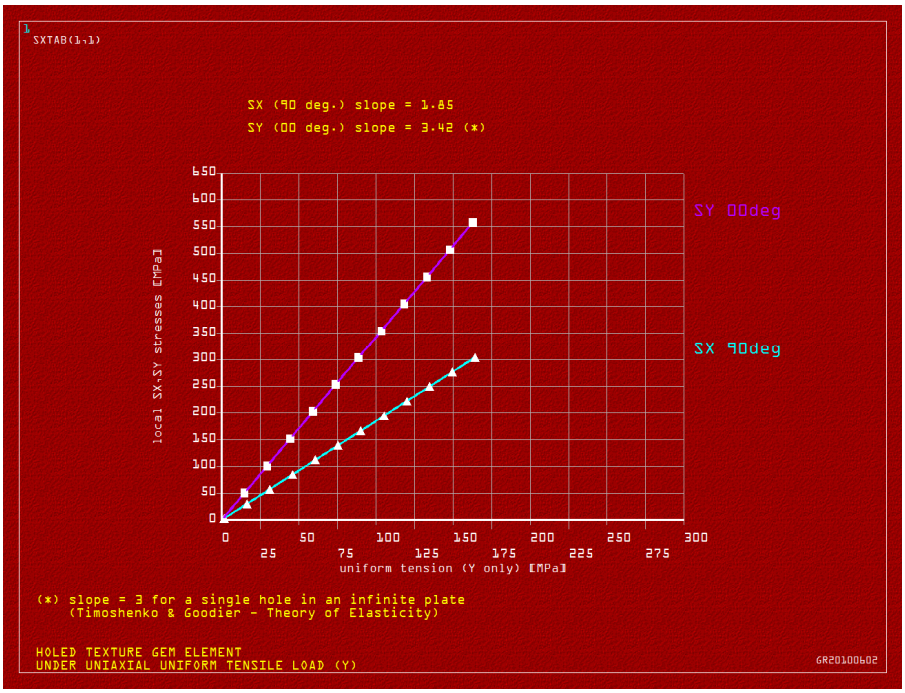

Fig. 1§1-7 Stress peaks varing the uniform tensile load along Y.

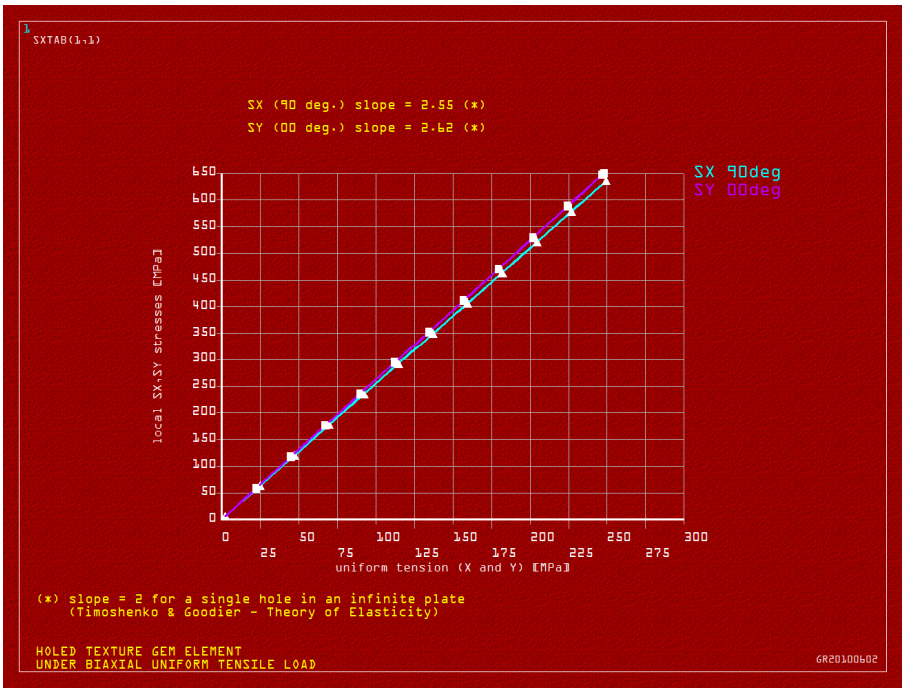

Fig. 1§1-8 Stress peaks varing the uniform biaxial tensile load.

The calculation of the stress concentration factors along directions lying in between cannot be solved by means of elementary mesh of the texture element and expensive analysis must be carried out on larger portions of the foil.

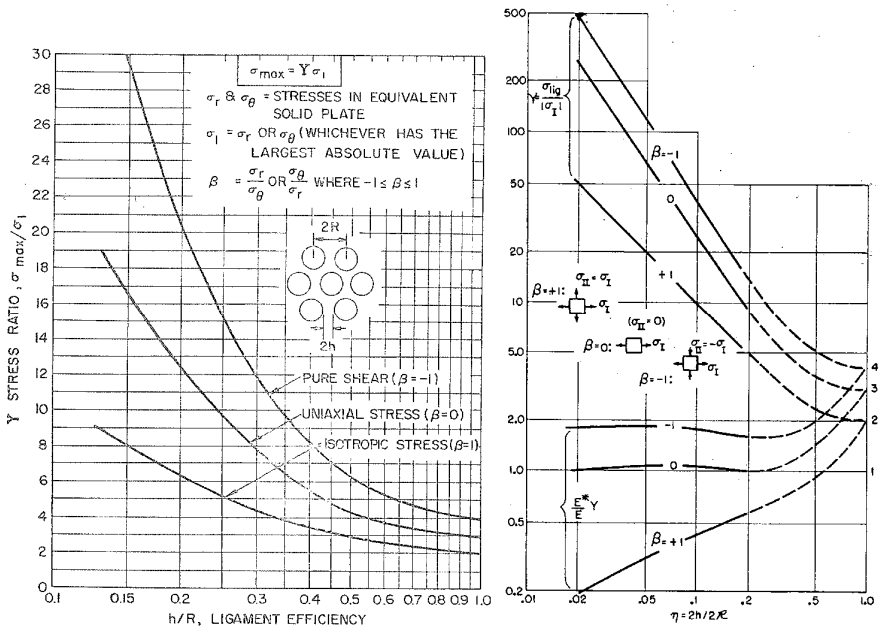

Fig. 1§1-9 O'Donnell [4] (on the left) and Horvay [2] (on the right) stress concentration factors; for the GEM foils the ligament efficiency is 0.5; the pure shear ($\beta = -1$; $Kxy^{\pi/2}\big|_{shear} = 4$ in [3]) is not taken into account.

The drawback of the stress concentration factors is that *a simultaneous tensioning along two orthogonal directions is needed to achieve extreme biaxial stresses without compromising the integrity of the GEM foils*; for instance if $\sigma_{yield} = 272.5$ MPa [h] for a 5 μm layer thickness of copper on kapton then the tensioning along X (Y) only gives $\sigma_x = K_x^{\pi/2}\sigma_{uniform,Cu} = 4.40 \cdot 86.5$ MPa $= 380.6$ MPa ($\sigma_y = K_y^{0}\sigma_{uniform,Cu} = 295.8$ MPa) well above the yield point; on the contrary a biaxial stepped tensioning gives $\sigma_x = K_{xy}^{\pi/2}\sigma_{uniform,Cu} = 2.55 \cdot 86.5$ MPa $= 220.6$ MPa , $\sigma_y = K_{xy}^{0}\sigma_{uniform,Cu} = 226.6$ MPa well below the yield point; if so the uniform biaxial tensioning may be up to $\sigma_{uniform,Cu} = 104$ MPa ; besides *the simultaneous tensioning avoids the growth of local high compressive stresses* (the sign of SCF) but not the shears (see Fig. 1§1-5).

---

[h] According to [5] $\sigma_{yield} = \sigma_0 + kt^{-n}$ where σ_0=116 MPa , k=335 MPaμm^{-n} , n=0.473 , $t = 5\mu$m .

It must be also underlined that the difference between $K_x^{\pi/2} = 4.40$ and $K_y^{0} = 3.42$ should be taken into account during uniaxial tensile tests on thin perforated strips prototypes carried beyond the yield point as well as in the design of uniaxially loaded cylinders such the KLOE-GEM detectors.

1§2 - Equivalent material of a perforated single layer foil in plane stress.

The example of the previous section gives also the equivalent mechanical properties; for the copper layer the data are taken from [5] ($E_{Cu} = 108800$ MPa , $\nu_{Cu} = 0.34$); thus both the equivalent Young modulus $E_{Cu,\,perf.}$ and the Poisson ratio $\nu_{Cu,\,perf.}$ can be easily computed from Fig. 1§1-1 (uniaxial loading on X), that is $E_{Cu,\,perf.} = \sigma_{uniform,\,Cu} / \bar{\varepsilon}_x|_x$ where $\bar{\varepsilon}_x|_{x\,=} 4|U_x|_x|/p$ and $U_x|_x = \pm 0.052565$ µm ; then $E_{Cu,\,perf.} = 57595.4$ MPa ; besides $\nu_{Cu,\,perf.} = -\bar{\varepsilon}_y|_x / \bar{\varepsilon}_x|_x$ where $\bar{\varepsilon}_y|_{x\,=} -4|U_y|_x|/\sqrt{3}p$ and $U_y|_x = \pm 0.031002$ µm (see note 1§1 - d); thus $\nu_{Cu,\,perf.} = |U_y|_x|/\sqrt{3}|U_x|_x|$ that is $\nu_{Cu,\,perf.} = 0.34051$; the same results can be obtained from Fig. 1§1-2 (uniaxial loading on Y), that is $E_{Cu,\,perf.} = \sigma_{uniform,\,Cu} / \bar{\varepsilon}_y|_y$ where $\bar{\varepsilon}_y|_{y\,=} 4|U_y|_y|/\sqrt{3}p$ and $U_y|_y = \pm 0.091045$ µm ; then $E_{Cu,\,perf.} = 57595.5$ MPa ; at the same time $\nu_{Cu,\,perf.} = -\bar{\varepsilon}_x|_y / \bar{\varepsilon}_y|_y$ where $\bar{\varepsilon}_x|_{y\,=} -4|U_x|_y|/p$ and $U_x|_y = \pm 0.017899$ µm (see note 1§1 - d); thus $\nu_{Cu,\,perf.} = \sqrt{3}|U_x|_y|/|U_y|_y|$ that is $\nu_{Cu,\,perf.} = 0.34051$.

Just for sake of completeness the values $\nu_{Cu,\,perf.} = 0.34051$, $E_{Cu,\,perf.} = 57595.5$ MPa can be checked in the biaxial state, that is $U_x|_{xy} = \pm p\sigma_{uniform,\,Cu}(1-\nu_{Cu,\,perf.})/4E_{Cu,\,perf.}$ and $U_y|_{xy} = \pm\sqrt{3}p\sigma_{uniform,\,Cu}(1-\nu_{Cu,\,perf.})/4E_{Cu,\,perf.}$; then $U_x|_{xy} = \pm 0.034666\ \mu$m (instead of $\pm 0.034670\ \mu$m ; see Fig. 1§1-3 and note 1§1 - d) and $U_y|_{xy} = \pm 0.060043\ \mu$m (instead of $\pm 0.060050\ \mu$m); this is a further confirmation of the *macroscopic isotropy* of the GEM foils. These results show that *the ratios* $E_{Cu,\,perf.}/E_{Cu} \cong 0.53$ *and* $\nu_{Cu,\,perf.}/\nu_{Cu} \cong 1$ *are again in very good agreement with* [4] [a] (see Fig. 1§2-1); these ratios can be extended to the kapton layer also since the its Poisson ratio is more or less the same; it must be

[a] O'Donnell data refer to equivalent mechanical properties for $\nu = 0.3$; for a ligament efficiency of 0.5 the ratios in Fig. 1§2-1 are equal to those found for the GEM foils (the data in [4] refer only to moderately thick plates; that limitation is insignificant in plane stress but not in bending); it is a little bit strange that those data (extrapolated from Sampson experimental measurements on plastic, $\nu = 0.5$) show a macroscopic anisotropy of the hexagonal perforated plates; that anisotropy regards the Poisson ratios (averaged by O'Donnell) that were found to be different along two orthogonal directions, but not the Young modulus; it is conceptually difficult to understand that experimental result because of the macroscopic isotropy due to the hexagonal symmetry; some numerical tests with $\nu_{Cu} = 0.3$ (instead of 0.34) and a ligament efficiency of 0.35 (instead of 0.5) give the ratios $E_{Cu,\,perf.}/E_{Cu} = 0.33$, $\nu_{Cu,\,perf.}/\nu_{Cu} = 1.19$ (that is $\nu_{Cu,\,perf.} = 0.357$) and $Kx^{\pi/2} = 6.47$, $Kxy^{0} = 3.45$ that again match very well the O'Donnell data; on the contrary tests with $\nu_{Cu} = 0.45$ give a lower equivalent Poisson ratio $\nu_{Cu,\,perf} = 0.4$ for a ligament efficiency of 0.35 (the Young modulus ratio is always 0.33); thus the O'Donnell data are in good agreement for Poisson ratios close to 0.3 (i.e. for copper and kapton in plane stress).

underlined that *the equivalent properties found by a plane stress similitude give a good approximation in plane stress problems but are not accurate in bending problems*, as Sampson experimental data on moderately thin plates.

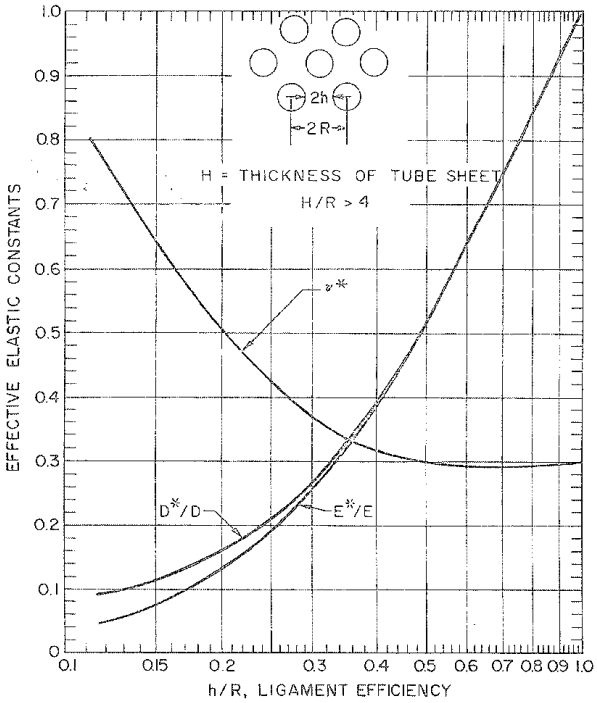

Fig. 1§2-1 O'Donnell equivalent elastic constants for perforated and relatively thick plates (ν=0.3 **)** [4]; these constants are not accurate in bending problems of relatively thin plates (Sampson)**.**

Furthermore *the ratios* $E_{Cu,\,perf.}/E_{Cu} \cong 0.53$ *and* $\nu_{Cu,\,perf.}/\nu_{Cu} \cong 1$ *agree with theoretical results of Day* [6] (see Fig. 1§2-2 where $\overline{p} = 0.77$, being $\overline{p} = 1 - f$, $f = \pi d^2/2\sqrt{3}p^2 = 0.23$ the holes area/total area fraction); on the contrary in [7] $E_{perf.}/E \cong 1/(1+3f) = 0.60$, $f = 0.23$ is slightly greater because the applied Airy stress function on the boundaries is simply taken from [3] and gives the so called "dilute solution" corresponding to very small solidity ratios only (i.e. the solution for a single hole in an infinite plate, see note 1§1 - g); thus the relations (1§2-1) hold for the GEM foils (both for kapton and copper layer).

$$E_{perf.}/E \cong 0.53 \qquad \nu_{perf.}/\nu \cong 1 \qquad \nu \cong 0.34 \qquad \textit{(plane stress only)} \tag{1§2-1}$$

In despite of the previous successful comparisons there is a much more important concept regarding with the strain energy that must be emphasized; Fig. 1§2-3 shows the strain energy of the $t_{Cu} = 5\ \mu$m Cu layer under $\sigma_{uniform,\,Cu} = 86.5$ MPa biaxial tensile load; the numerical integration over the volume gives $W_{biaxial,\,Cu} = 0.364\text{E}-05$ mJ ; the macroscopic strain energy is $W_{biaxial,\,Cu} = \sigma_{uniform,\,Cu}(\overline{\varepsilon}_x\big|_{xy} + \overline{\varepsilon}_y\big|_{xy})\sqrt{3}p^2 t_{Cu}/8$ where

$\bar{\varepsilon}_x\big|_{xy} = 4\big|U_x\big|_{xy}\big|/p$, $\bar{\varepsilon}_y\big|_{xy} = 4\big|U_y\big|_{xy}\big|/\sqrt{3}p$, $U_x\big|_{xy} = \pm 0.034670\ \mu\text{m}$, $U_y\big|_{xy} = \pm 0.060050\ \mu\text{m}$, being $\sqrt{3}p^2 t_{Cu}/4$ the volume; then $W_{biaxial,\,Cu} = \sigma_{uniform,\,Cu}(\sqrt{3}\big|U_x\big|_{xy}\big| + \big|U_y\big|_{xy}\big|)pt_{Cu}/2$ that is $W_{biaxial,\,Cu} = \sigma_{uniform,\,Cu}\sqrt{3}\big|U_x\big|_{xy}\big|pt_{Cu}$ if $\big|U_y\big|_{xy}\big| = \sqrt{3}\big|U_x\big|_{xy}\big|$; thus $W_{biaxial,\,Cu} = 0.364\text{E}-05\ \text{mJ}$ again; for uniaxial loads (not presented for conciseness) $W_{uniaxial-X,\,Cu} = W_{uniaxial-Y,\,Cu}$.

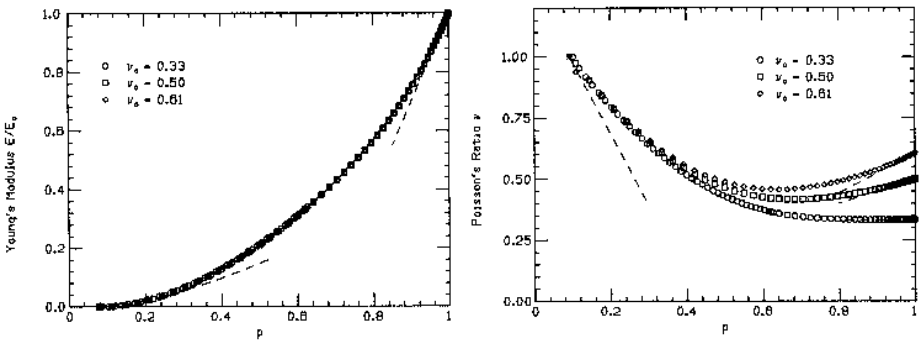

Fig. 1§2-2 Day [6] simulations for Young modulus and Poisson ratio for a regular array of circular holes in a triangular arrangment; the most important conclusion of that work is that *"the ratio* $E_{perf.}/E$ *is the same for all materials and independent of the Poisson ratio for any prescribed geometry…"* as the numerical tests in note 1§2 - a have showed, that is $E_{perf.}/E$ *depends only on the ligament efficiency*; these simulations were compared with uniaxial tensile experiments only.

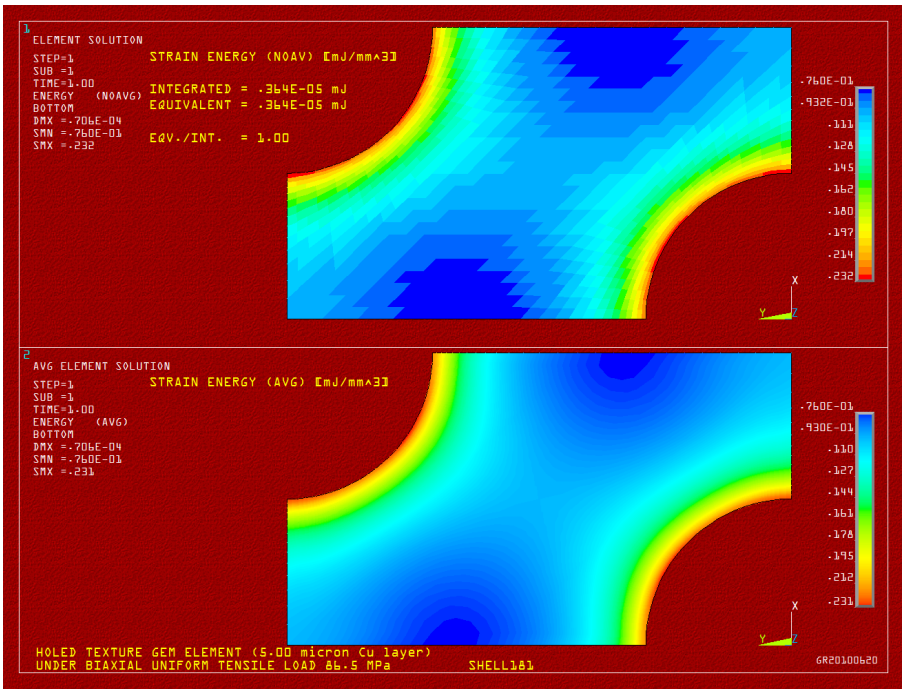

Fig. 1§2-3 Strain energy of the 5 µm Cu layer under $\sigma_{uniform,\,Cu}$ = 86.5 MPa biaxial tensile load.

In the same way, if $\sigma_{uniform,\,kap.} = 2.7$ MPa and $t_{kap.} = 50\ \mu$m , then the strain energy of kapton layer is $W_{biaxial,\,kap.} = 0.113\text{E}-05$ mJ under the same biaxial displacements.

It follows that the relations (1§2-1) are derived assuming that *the strain energy of the perforated foil equates that of the equivalent material under the same load*; this is a general concept that will be applied on the bending problems also [b]; even if its effectiveness is accepted without any proof (it is not the subject of the present work) there are many hints revealing it really works on an hexagonal symmetry; furthermore the Backus averaging formulas [c] for any multilayered material can be derived in similar fashion (i.e. by means of a strain energy balance) as shown in (1§2-2) to (1§2-4) where $\alpha = t^{(1)}/(t^{(1)}+t^{(2)})$ is the *volume fraction*; then *the strain energy comparison is fundamental in the homogenization of a multilayered perforated foil*.

$$E^{(eq.)} = \frac{2\beta'\beta''}{\beta'+\beta''} \qquad \nu^{(eq.)} = \frac{\beta'-\beta''}{\beta'+\beta''} \qquad \mu^{(eq.)} = \beta''/2$$
$$\beta' = \alpha\frac{E^{(1)}}{1-\nu^{(1)}} + (1-\alpha)\frac{E^{(2)}}{1-\nu^{(2)}} \qquad \beta'' = \alpha\frac{E^{(1)}}{1+\nu^{(1)}} + (1-\alpha)\frac{E^{(2)}}{1+\nu^{(2)}} \tag{1§2-2}$$

$$\frac{\nu_z^{(eq.)}}{1-\nu^{(eq.)}} = \alpha\frac{\nu_z^{(1)}}{1-\nu^{(1)}} + (1-\alpha)\frac{\nu_z^{(2)}}{1-\nu^{(2)}} \qquad \delta = \frac{E_z}{(1-\nu)E - 2\nu_z^2 E_z} \tag{1§2-3}$$

$$\frac{1}{(1-\nu^{(eq.)})E^{(eq.)}}\left(\frac{1}{\delta^{(eq.)}}\right) = \alpha\frac{1}{(1-\nu^{(1)})E^{(1)}}\left(\frac{1}{\delta^{(1)}}\right) + (1-\alpha)\frac{1}{(1-\nu^{(2)})E^{(2)}}\left(\frac{1}{\delta^{(2)}}\right)$$
$$1/\mu_z^{(eq.)} = \alpha/\mu_z^{(1)} + (1-\alpha)/\mu_z^{(2)} \tag{1§2-4}$$

Note that in general the Backus averaging (1§2-2), (1§2-3), (1§2-4) should be performed before the perforation homogenization (1§2-1); in the present case, where the rule of mixtures holds, that sequence can be reversed.

---

[b] The integration of the strain energy over the volume is simple for solid elements since the product $\sigma\,\varepsilon$ is constant in each; on the contrary the integration for shell elements must take into account at least a linear variation of both σ and ε through the thickness; a dedicated macro was written for this aim.

[c] Appendix A is a brief summary of the Backus averaging that was applied only on two layers since the tri-layered GEM foils are transversely symmetrical.

1§3 - Equivalent material of a perforated tri-layer foil in plane stress.

Up to now only a single layer was examined; the mechanical properties of a multilayered material can be replaced by those of an "equivalent material"; the process of averaging in elasticity is not unique and is limited to the weighting of the mechanical properties of the bulk materials by means of proper hypothesis to fulfil peculiar problems; the Backus averaging has been tested separately in many different simulations and gives very good results in the plane stress problems; it was selected among many others since it is complete from theoretical point of view and it is simple; furthermore the Backus averaging takes into account the transversely isotropy of each layer as well as the mismatch of the Poisson ratio and the shear modulus other than the Young.

As far as the GEM foils the process of averaging is greatly simplified if only the difference of the Young modulus between copper and kapton is taken into account; then the so-called *rule-of-mixtures* (1§3-1) holds.

$$E_{eq.} = \alpha E_{kap.} + (1-\alpha) E_{Cu} \qquad \nu_{eq.} = \nu_{kap.} = \nu_{Cu} \qquad \textit{(rule of mixtures)} \qquad (1\S3\text{-}1)$$

Nevertheless it must be underlined that if some other mechanical property "jumps" across the thickness then the rule-of-mixtures does not hold anymore; furthermore each single thin foil of any material always exhibits at least transversal isotropy features itself separately before bonding or depositing as for kapton [8]; if $\alpha = t_{kap.}/(t_{kap.} + t_{Cu}) = 5/6$ is the *volume fraction* of the GEM foils, $t_{kap.} = 50\ \mu\text{m}$, $t_{Cu} = 10\ \mu\text{m}$ (5+5) and if [5] $E_{kap.} = 3400$ MPa, $\nu_{kap.} = 0.34$ then $E_{eq.} = 20966.7$ MPa and from (1§2-1) then (1§3-2).

$$E_{eq.,\,perf.} = 11112.4 \text{ MPa} \qquad \nu_{eq.,\,perf.} = 0.34 \qquad \textit{(plane stress only)} \qquad (1\S3\text{-}2)$$

The Young modulus in (1§3-2) is more than twice of that reported in [9] and should explain the discrepancy between numerical and experimental results.

A numerical simulation by means of solid elements (fully 3D) was also performed in order to prove (1§3-2). The texture GEM element shown in Fig. 1§3-1 is submitted to a biaxial stress equal to $\sigma_{uniform} = 16.7$ MPa [a] imposing the displacements obtained from the shell elements (note 1§1 - b); the stresses are underestimated a little (Fig. 1§1-4).

---

[a] That value corresponds to $S = 1$ N/mm tensioning given in [10] for a $60\ \mu$m thick GEM foil (50 + 5 + 5; 300 mm x 700 mm); then the copper layer is subjected to $\sigma_{uniform,\,Cu} = 86.5$ MPa (as in previous sections) and the kapton one to $\sigma_{uniform,\,kap.} = 2.7$ MPa, if $\sigma_{uniform} = \alpha\sigma_{uniform,\,kap.} + (1-\alpha)\sigma_{uniform,\,Cu}$, α=5/6; the value of $\sigma_{uniform} = 16.7$ MPa is given by the nodal forces balance on boundaries and it is not applied straightforwardly.

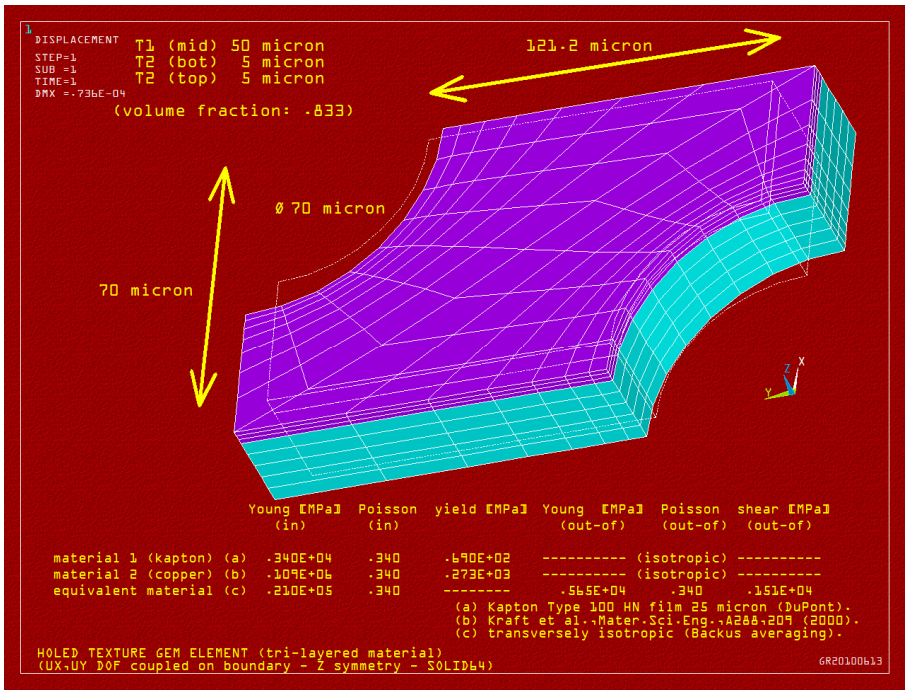

Fig. 1§3-1 Half of the tri-layered GEM foil (not refined mesh due to number of elements limitation).

Fig. 1§3-2 shows the stresses and the strain energy of the "real material" under the biaxial tensioning while Fig. 1§3-3 the same things but of the "equivalent material" (in Appendix A are given the basic formulas to reconstruct the real stresses starting from the equivalent ones); from these pictures it is possible to see that *the averaging spreads over the thickness stresses and energies of the more rigid material* (i.e. copper).

These results confirm (1§2-1) and (1§3-2) also from the strain energy point of view (and not only from the stresses via the displacements); a numerical integration of the strain energy gives the value of $W_{biaxial,\,GEM} = 0.422\text{E}-05\ \text{mJ}$ both of the "real material" and the "equivalent" one as expected [b]; that value refers only to half of the tri-layered foil (Z symmetry) and then $W_{biaxial,\,GEM} = (2W_{biaxial,\,Cu} + W_{biaxial,\,kap.})/2$ that exactly matches the values found in 1§2 - section; the results related to the uniaxial loadings are not reported and they agree very well also; some numerical tests on materials having unequal Poisson ratio and shear modulus give also very good results.

[b] It is a numerical proof of the exactness of the averaging.

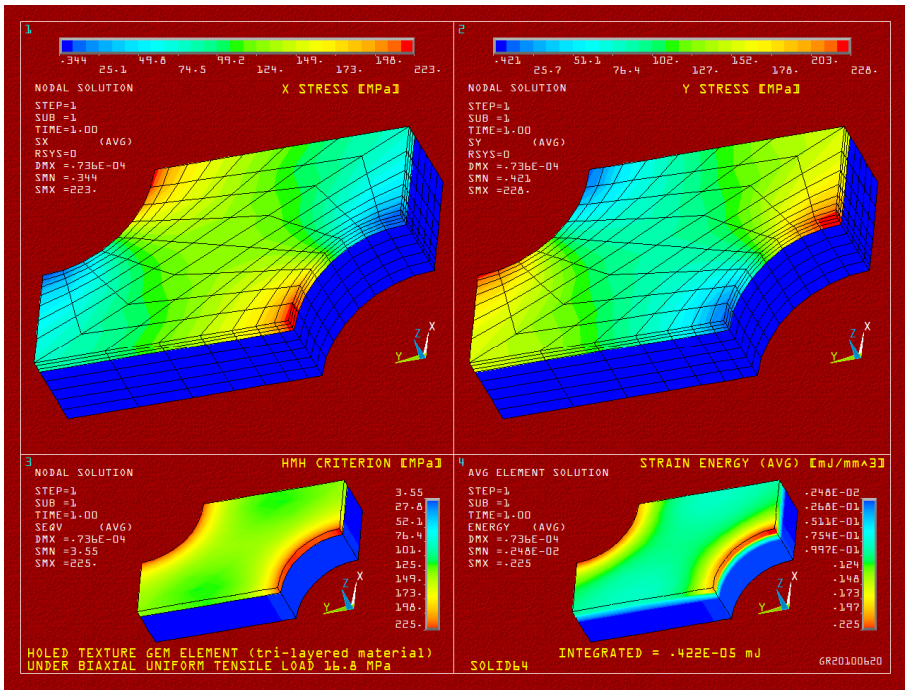

Fig. 1§3-2 Stresses and strain energy of the tri-layered GEM material under $\sigma_{uniform} = 16.7$ MPa biaxial load**.**

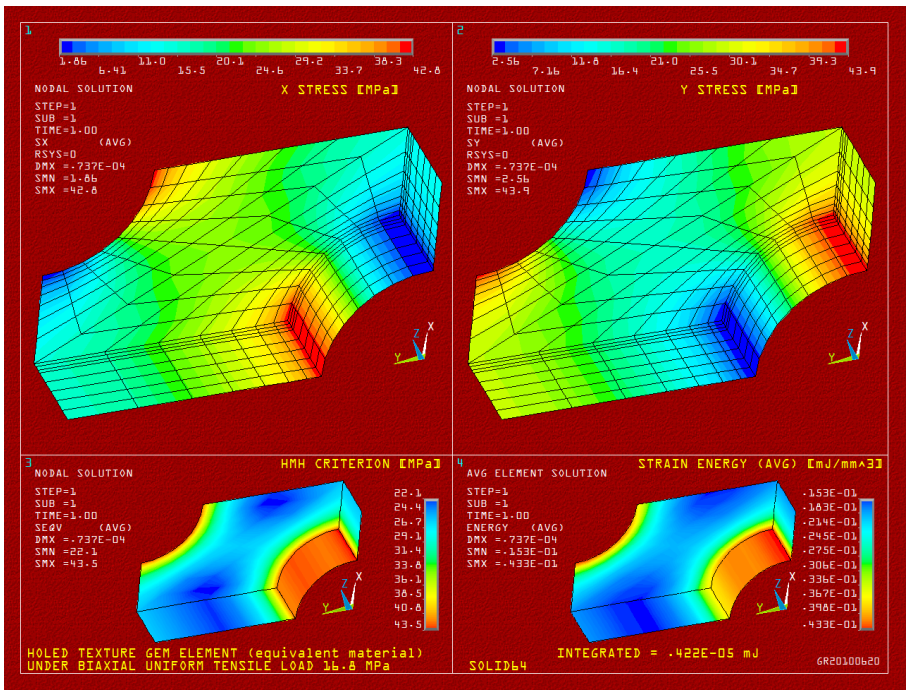

Fig. 1§3-3 Stresses and strain energy of the equivalent material under $\sigma_{uniform} = 16.7$ MPa biaxial load.

2 - The bending homogenization.

Numerical test on bending of non-perforated tri-layered GEM plates show that the equivalent mechanical properties given by the "rule-of-mixtures" greatly overestimate the displacements (sometimes much more than a factor of 2 if considering the Backus averaging, that includes the transversal properties); it follows that *the non-perforated GEM foils are more stiff in bending than in tensioning*; that disagreement is due to that the averaging does not take into account the distribution through the thickness of the flexural rigidities of the layers (in the GEM foils the top and bottom copper layers carry the most of the bending load and are at the same time the more rigid); then the first step is to determine the flexural rigidity $D_{eq.}$ of the equivalent material that replaces the rule-of-mixtures; the second step deals with the perforation. Since the bending stresses in GEM foils are negligible then the attention will be focused on the displacements only.

2§1 - Equivalent material of non-perforated tri-layer foil in bending.

The factor of 2 gives a quick estimation of the ratio of the flexural rigidities between the real material and the equivalent one given by the Backus averaging; but that ratio is meaningless since that averaging does not work properly in bending; then it is more correct to determine an absolute value of the equivalent flexural rigidity rather than a ratio.

The flexural rigidity of the equivalent material $D_{eq.}$ can be computed numerically by comparing the displacements of simple bodies of the real tri-layered material (as strips, plates, beams and so on) to those given by analytical solutions of the homogenized material under the same loads. There are many ways to do it but one of the simplest and well suited is that of a simply supported strip of length l [mm] submitted both to a transversal load q [N/mm²] and a tensile force S [N/mm] [11]; in (2§1-1) f [mm] is the mid displacement and u a dimensionless parameter.

$$\left(\frac{4Sf}{ql^2}\right)=\frac{\operatorname{sech} u-1+u^2/2}{u^2} \qquad \text{where} \qquad u^2=\frac{Sl^2}{4D_{eq.}} \tag{2§1-1}$$

The trivial computation of $D_{eq.}$ is not free of contradictions as it can appear at first sight: a numerical simulation of the simply supported strip of the real material gives the displacement f; then the LHS of (2§1-1) is known, then u and $D_{eq.}$. Once $D_{eq.}$ in determined a new simulation is performed in order to check if the equivalent material gives the same displacement f and the same elongation under the same loads q and S.

It can be easily understood that the results are not consistent, since $D_{eq.}$ usually meets the displacement f but not the elongation (even if playing with the Poisson ratio) and it is not unique under different conditions; then any calculated equivalent flexural rigidity $D_{eq.}$ is circumscribed to a small range of the given loads and must averaged in some way to approximate both displacements and elongations [a]; thus the homogenization of a tri-layered material subjected to both bending and tensioning is rather difficult; *fortunately this is not the case of the GEM foils* since the non-dimensional parameter u in (2§1-1) takes extremely large values.

$$\lim_{u\to+\infty}\frac{\operatorname{sech} u-1+u^2/2}{u^2}=\frac{1}{2}\quad\Rightarrow\quad f\cong\frac{1}{8}\frac{ql^2}{S} \tag{2§1-2}$$

It follows that the GEM foil behaves like a cable; the expression (2§1-2) gives a much more remarkable information, i.e. *an accurate material characterization of the GEM foil in bending is not needed since its sag is independent on the flexural stiffness*.

Thus the bending homogenization is not introduced at all even if its analysis is very interesting especially in that "grey zone" where the tensile stresses are of the same order of magnitude of the bending ones.

It must be underlined that (2§1-2) is an upper bound, that is if the foil is stretched along the other two edges also, its sag will be surely lower than $ql^2/8S$; just to write some numbers [10] assuming $q=1.21\text{E-}06$ N/mm^2 [b], $l=300$ mm, $S=1$ N/mm then $f<13.6$ μm.

In order to determine an approximate value of $D_{eq.}$ the relation (2§1-1) can be used only in very small scale models where the bending effects become dominant; roughly $D_{eq.}\cong 1$ Nmm is obtained for a simply supported non-tensioned strip ($S=0$); no further investigations on the bending stiffness have been carried out since they are meaningless.

The sag f of a rectangular membrane [3] [c] is given by (2§1-3) where l, w are respectively length, width in mm; the equation (2§1-3) is equal to (2§1-2) as $w\to+\infty$.

$$f=\frac{ql^2}{8S}\left[1-\frac{32}{\pi^3}\sum_{n=1}^{+\infty}\frac{(-1)^{n+1}}{(2n-1)^3}\operatorname{sech}\frac{(2n-1)\pi}{2}\left(\frac{w}{l}\right)\right] \tag{2§1-3}$$

---

[a] The introduction of an "equivalent thickness" should be a remedy.

[b] $q=\bar{p}\rho_{eq}g(t_{kap.}+t_{Cu})$ where $g=9.80665$ m/s^2, $t_{kap.}+t_{Cu}=0.06$ mm, $\rho_{eq}=\alpha\rho_{kap.}+(1-\alpha)\rho_{Cu}$, $\alpha=5/6$, $\bar{p}=0.77$ the effective area/total area fraction, $\rho_{kap.}=1420$ kg/m^3, $\rho_{Cu}=8900$ kg/m^3; q is the own weight and can be increased or replaced by some other load such the electrostatic one (about 1 Pa).

[c] The solution in [3] seems to be incorrect about the sign of the alternating terms and was slightly modified.

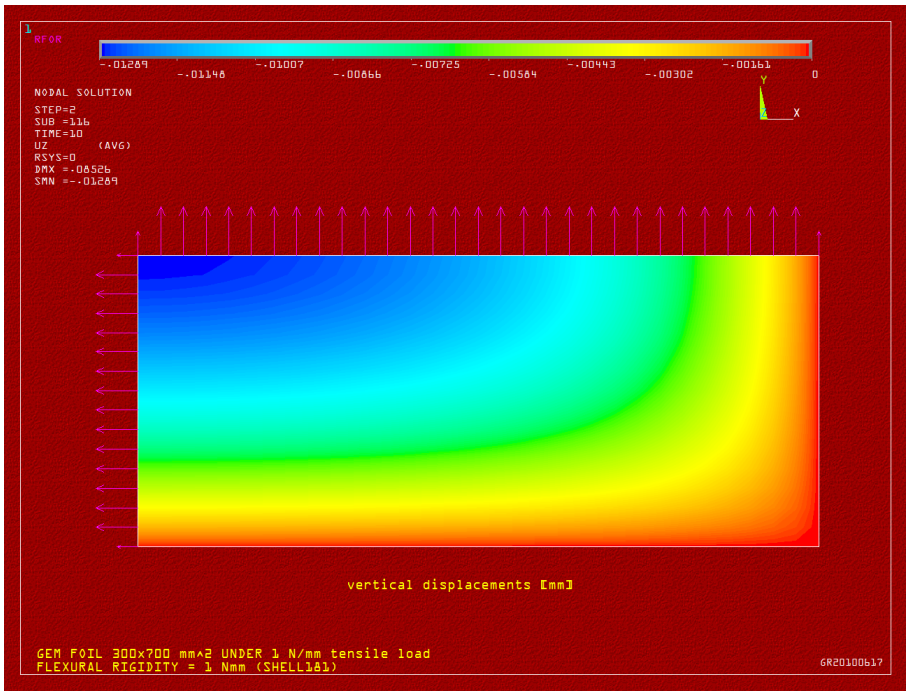

Fig. 2§1-1 GEM foil sag (own weight only) under $S = 1$ N/mm biaxial load (bending stiffness 1 Nmm) .

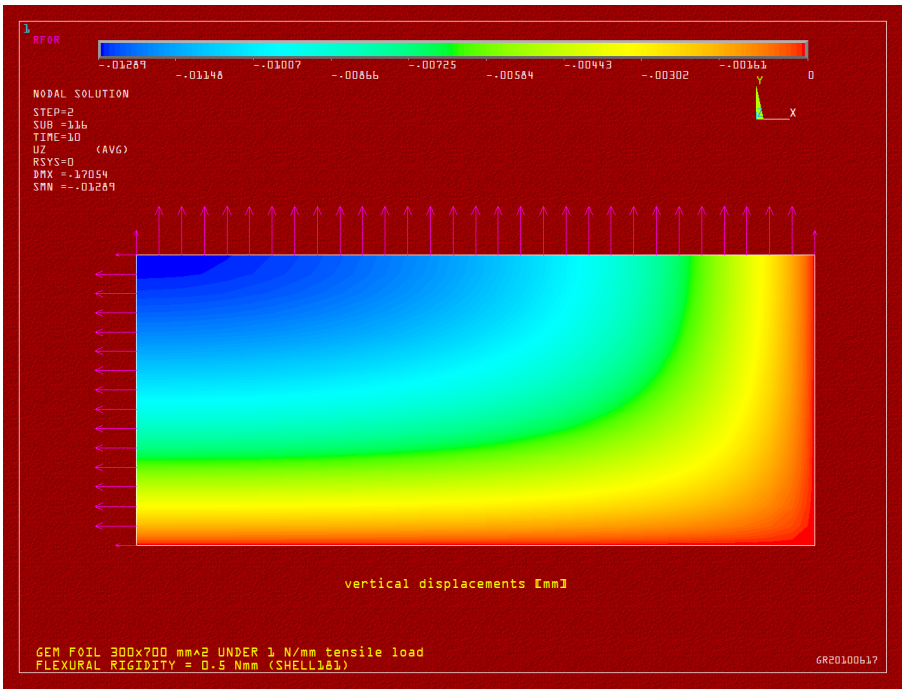

Fig. 2§1-2 Same as Fig. 2§1-1 but bending stiffness 0.5 Nmm (the sag error in bending should be 100%).

Since (2§1-3) converges rapidly if $w > l$ then the sag f_1 (2§1-4) is given taking only the first term of the series; if $w = 700$ mm then $f_1 \cong 12.9$ μm.

$$f_1 \cong \frac{ql^2}{8S}\left[1-\frac{32}{\pi^3}\operatorname{sech}\ \frac{\pi}{2}\left(\frac{w}{l}\right)\right] \qquad (w > l) \qquad (2\S1\text{-}4)$$

Fig. 2§1-1 gives exactly the same sag of 12.9 μm equal to f_1 in (2§1-4); Fig. 2§1-2 gives the same sag also but with one half of the flexural stiffness showing that the displacements are independent on the material characterization. Thus *any numerical analysis concerning the sag of any large area GEM square foil is unnecessary*.

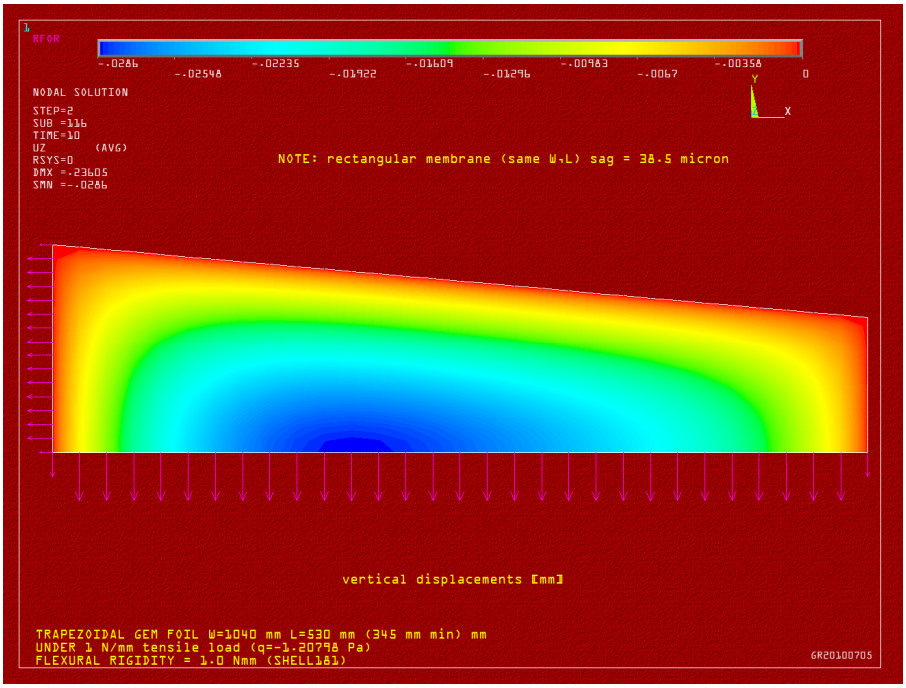

Fig. 2§1-3 Trapezoidal membrane sag (own weight only) under $S = 1$ N/mm biaxial load.

As far as a trapezoidal membrane the conclusions are not much different; for instance, if $w = 1040$ mm and $l = 530$ mm, the sag (2§1-4) due the own weight only corresponding to $S = 1$ N/mm is $f_1^{upper} \cong 38.5$ μm which is the upper bound for the trapezoidal membrane; furthermore (2§1-4) gives the lower bound also for the same membrane; then *any trapezoidal membrane has sags included in the range given by* (2§1-4) as shown in Fig. 2§1-3 where $f \cong 28.6$ μm is the sag due to the own weight (the lower bound is computed assuming $w = 1040$ mm and $l = 345$ mm; then $f_1^{lower} \cong 17.7$ μm i.e. $17.7\ \mu\text{m} < f < 38.5\ \mu\text{m}$; roughly f is more or less the arithmetic mean: $28.6\ \mu\text{m} \cong (17.7\ \mu\text{m} + 38.5\ \mu\text{m})/2 = 28.1\ \mu\text{m}$).

2§2 - Equivalent material of perforated single layer foil in pure bending.

This section can be skipped as the previous conclusions; nevertheless there is still a merely academic question concerning the macroscopic isotropy of the GEM foil in pure bending also; the following analysis is focused on a single layer only and will show the equality between the strain energies related to orthogonal directions of bending.

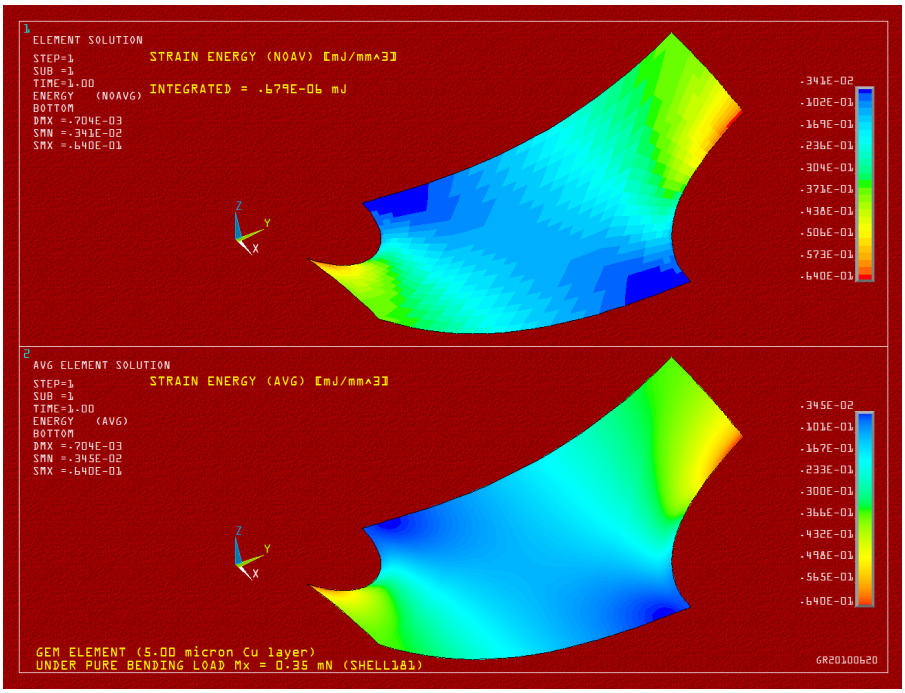

Fig. 2§2-1 Strain energy of 5 µm Cu layer under 0.35 mN pure bending in X.

The procedure is similar to that adopted in plane stress; $M_{uniform,\,Cu} = 0.35$ mN is the remote bending load in X and the trial and error procedure described in note1§1 - b gives a rotation of $\varphi_x = 27.8$ mrad (imposing the nodal moments balance); the same bending moment $M_{uniform,\,Cu}$ applied in Y gives $\varphi_y = 16.1$ mrad , i.e. $\varphi_x/\varphi_y = \sqrt{3}$; Fig. 2§2-1 and Fig. 2§2-2 shows that the integrated strain energy is equal in both cases, that is $W_{bending-X,\,Cu} = W_{bending-Y,\,Cu} = 0.679$E-06 mJ .

Thus that result confirms that *the GEM foils are macroscopically isotropic in bending also*; it must be underlined that this does not mean that they are fully isotropic since the *engineering parameters* cannot be reduced to only two (Young & Poisson).

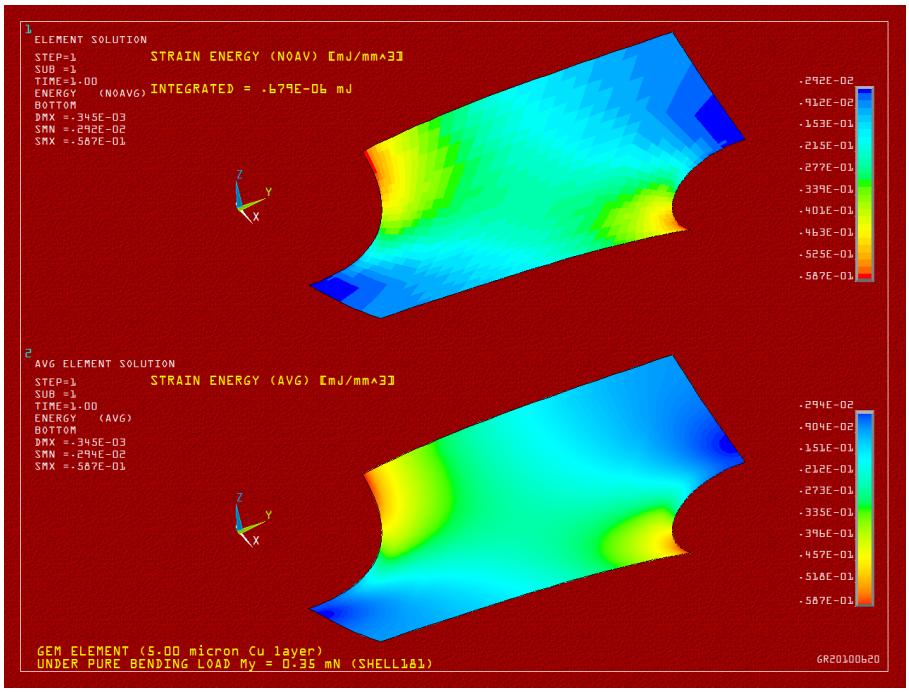

Fig. 2§2-2 Strain energy of 5 μm Cu layer under 0.35 mN pure bending in Y.

The macroscopic strain energy is $W_{bending,\,Cu} = 2D_{Cu,\,perf.}\,\varphi_x^{\,2}/\sqrt{3} = 2D_{Cu,\,perf.}\,\varphi_y^{\,2}\sqrt{3}$ and equating to $W_{bending,\,Cu} = 0.679\text{E-}06$ mJ it follows that $D_{Cu,\,perf.} = 0.76\text{E-}03$ Nmm , i.e. $D_{Cu,\,perf.}/D_{Cu} \cong 0.59$, being $D_{Cu} = E_{Cu}\,t_{Cu}^{\,3}/12(1-\nu_{Cu}^{\,2})$ the flexural stiffness; in general the ratio $D_{perf.}/D \cong 0.59$ is a little bit greater than $E_{perf.}/E \cong 0.53$ (1§2-1) and thus *also the perforated GEM foils are more stiff in bending than in tensioning*.

3 - Concluding remarks.

Some subjects should be analyzed with deeper simulations and experimental tests; first of all the mechanical characterizations of the non perforated materials are given in [5] but there are some open questions about the Young modulus and the Poisson ratio of the copper layer as well as the yield strength [a].

It is well known that the copper/kapton multi-layers can carry loads higher than the yield bounds of bulk materials without appreciable permanent deformations; that feature cannot be easily extended to the perforated foils since the plasticization area begins to grow just around the holes (i.e. just on the free circular edges where crack and de-bonding easily occur depending on the quality of the etching; for instance the previous SCF are computed for a perfect circular profile of the hole and sharp micro-imperfections along it are potentially dangerous as far as any crack propagation even at low stresses).

Thus the tensile loads in perforated foils can exceed the yield bounds leaving the foil perfectly elastic from a macroscopic point of view (in a biaxial tensioning the copper plastic zones look like rings leaving most of the ligaments elastic) but the local permanent deformations may be unacceptable.

At the present time a plastic analysis is unnecessary since the sags seems to be acceptable even for large area foils in a perfectly elastic regime; if the yield strengths reveal to be in some way lower than those suggested in literature then only dedicated experimental tests as well as numerical plastic analysis may indicate the upper bounds of the tensile loads.

A creep analysis is also not so stringent since the kapton layer is extremely stable for long time loads in pure elasticity; on the contrary it should be taken into account in a wide plastic regime.

A modal analysis can be easily carried out since the membrane-type behavior (analytical solutions should be available in literature) to check resonances.

If a simultaneous tensioning is taken into account then local buckling and de-lamination due to compressive stresses are avoided; on the contrary these are two additional subjects to be investigated as well as the wrinkling.

---

[a] The copper Young modulus in [5] is averaged through the thickness but it is much more greater at the interface (because of the <111> dominant crystallographic texture) where also the Poisson ratio gets the greater value of 0.45; then there is a remarkable mismatch of the Poisson ratio between copper and kapton at the interface; the mismatch induces an unbalanced biaxial stress even in uniaxial tensile loads on very thin specimens that may be followed by wrinkling; the corresponding stress-strain fields are more complicated and the copper layer should be divided into two sub-layers at least.

4 - Appendix A

4§1 - Compliance and stiffness matrix of a TI material.

The compliance matrix $\mathbf{D}^{-1}$ (4§1-1) is given in terms of the five parameters (the so-called *engineering parameters*) E , E_z (*in-plane* and *out-of-plane* Young), ν , ν_z [a] (*in-plane* and *out-of-plane* Poisson) and G_z (*out-of-plane* shear) being $1/G = 2\left(1/E + \nu/E\right)$ (*in-plane* shear), $\boldsymbol{\sigma}$, $\boldsymbol{\varepsilon}$ (stress and strain vector), $\boldsymbol{\varepsilon} = \mathbf{D}^{-1}\boldsymbol{\sigma}$ and the symmetry axis z .

$$\begin{pmatrix} \varepsilon_x \\ \varepsilon_y \\ \varepsilon_z \\ \gamma_{yz} \\ \gamma_{xz} \\ \gamma_{xy} \end{pmatrix} = \begin{pmatrix} 1/E & -\nu/E & -\nu_z/E & 0 & 0 & 0 \\ & 1/E & -\nu_z/E & 0 & 0 & 0 \\ & & 1/E_z & 0 & 0 & 0 \\ & & & 1/G_z & 0 & 0 \\ & \text{sym.} & & & 1/G_z & 0 \\ & & & & & 1/G \end{pmatrix} \begin{pmatrix} \sigma_x \\ \sigma_y \\ \sigma_z \\ \tau_{yz} \\ \tau_{xz} \\ \tau_{xy} \end{pmatrix} \qquad (4\S1\text{-}1)$$

Then the stiffness matrix $\mathbf{D}$ (4§1-2) is given in terms of the five constants D_{11} , D_{12} , D_{13} , D_{33} , D_{44} being $D_{66} = \left(D_{11} - D_{12}\right)/2 = G$, $\boldsymbol{\sigma} = \mathbf{D}\boldsymbol{\varepsilon}$.

$$\begin{pmatrix} D_{11} & D_{12} & D_{13} & 0 & 0 & 0 \\ & D_{11} & D_{13} & 0 & 0 & 0 \\ & & D_{33} & 0 & 0 & 0 \\ & & & D_{44} & 0 & 0 \\ & \text{sym.} & & & D_{44} & 0 \\ & & & & & D_{66} \end{pmatrix} \quad \begin{array}{ll} D_{11} = \delta\dfrac{E - \nu_z^2 E_z}{\left(1+\nu\right)E_z}E & D_{12} = \delta\dfrac{\nu E + \nu_z^2 E_z}{\left(1+\nu\right)E_z}E \\ D_{13} = \delta\nu_z E & D_{33} = \delta\left(1-\nu\right)E \\ D_{44} = G_z & \delta = \dfrac{E_z}{\left(1-\nu\right)E - 2\nu_z^2 E_z} \end{array} \qquad (4\S1\text{-}2)$$

The inverse relations are given in (4§1-3) where B , $E_b = E/\left(1-\nu\right)$ are respectively the bulk and biaxial modulus.

---

[a] ν_z=ν_{xz} is the *out-of-plane* major Poisson ratio (and ν_{zx}=$\nu_z E_z/E$ the minor) if E_z<E ; conversely (i.e. if E_z>E) ν_z is the minor (and $\nu_z E_z/E$ the major); ν is the *in-plane* Poisson ratio.

$$E=\left(D_{11}-D_{12}\right)\left(1-\frac{D_{13}^2-D_{12}D_{33}}{D_{11}D_{33}-D_{13}^2}\right)\quad E_z=D_{33}-\frac{2D_{13}^2}{D_{11}+D_{12}}\quad E_b=D_{11}+D_{12}-\frac{2D_{13}^2}{D_{33}}$$
$$B=\frac{E}{2\left(1-\nu-2\nu_z\right)+E/E_z}=\frac{D_{11}D_{33}+D_{12}D_{33}-D_{13}^2}{2D_{33}+D_{11}+D_{12}-4D_{13}} \tag{4§1-3}$$

A more readable expression of the stiffness matrix **D** (4§1-4) is written by means of the five parameters λ, μ_T, μ_L, φ, ψ being $\mu_T=G$, $\mu_L=G_z$; note that if $E_z=E$, $\nu_z=\nu$, $\mu_L=\mu_T=G$ (first Lamè constant) then $\lambda=\nu E/\left(1+\nu\right)\left(1-2\nu\right)$ (second Lamè constant) and $\varphi=\psi=0$.

$$\lambda=\frac{\left(\nu E+\nu_z^2E_z\right)}{\left(1-\nu\right)E-2\nu_z^2E_z}\cdot\frac{E}{\left(1+\nu\right)}\quad \varphi=\frac{\nu_z\left(1+\nu-\nu_z\right)E_z-\nu E}{\left(1-\nu\right)E-2\nu_z^2E_z}\quad \psi=\frac{\left(1-\nu^2+\nu_z^2\right)E_z-E}{E-\nu_z^2E_z}$$

$$\begin{pmatrix}\sigma_x\\ \sigma_y\\ \sigma_z\\ \tau_{yz}\\ \tau_{xz}\\ \tau_{xy}\end{pmatrix}=\begin{pmatrix}\lambda+2\mu_T & \lambda & \lambda+2\varphi\mu_T & 0 & 0 & 0\\ & \lambda+2\mu_T & \lambda+2\varphi\mu_T & 0 & 0 & 0\\ & & \lambda+2\left(1+\psi\right)\mu_T & 0 & 0 & 0\\ & & & \mu_L & 0 & 0\\ & \text{sym.} & & & \mu_L & 0\\ & & & & & \mu_T\end{pmatrix}\begin{pmatrix}\varepsilon_x\\ \varepsilon_y\\ \varepsilon_z\\ \gamma_{yz}\\ \gamma_{xz}\\ \gamma_{xy}\end{pmatrix} \tag{4§1-4}$$

A further expression of the stiffness matrix **D** (4§1-5) is given in terms of the five parameters λ, μ_T, μ_L, α, β where $\alpha=2\varphi\mu_T$, $\beta=2\mu_T\left(2-2\varphi+\psi\right)-4\mu_L$; ($\alpha=\beta=0$ when $\varphi=\psi=0$).

$$\begin{pmatrix}\lambda+2\mu_T & \lambda & \lambda+\alpha & 0 & 0 & 0\\ & \lambda+2\mu_T & \lambda+\alpha & 0 & 0 & 0\\ & & \lambda+2\alpha+\beta+4\mu_L-2\mu_T & 0 & 0 & 0\\ & & & \mu_L & 0 & 0\\ & \text{sym.} & & & \mu_L & 0\\ & & & & & \mu_T\end{pmatrix} \tag{4§1-5}$$

Since the strain energy is a quadratic form (i.e. $\forall\boldsymbol{\varepsilon}\neq 0, E_{strain}=\left(1/2\right)\boldsymbol{\varepsilon}^T\mathbf{D}\boldsymbol{\varepsilon}>0$) then the stiffness matrix **D** (as well as the compliance $\mathbf{D}^{-1}$) must be positive, that is all its principal minors $M_i, i=1,...,6$ (4§1-6) must be positive; it follows that $D_{11}>0$, $D_{33}>0$, $D_{44}>0$, $D_{66}>0$, $D_{11}>D_{66}$, $D_{13}^2<D_{33}\left(D_{11}-D_{66}\right)$. Assuming that all the above mentioned *engineers parameters* are positive then the constraints due to the strain energy of a TI material lead to $\nu_z^2<\left(1-\nu\right)E/\left(2E_z\right)$ that is $\delta>0$ ($-1<\nu<1/2$ isotropic).

$$\begin{aligned} M_1 &= D_{11} > 0 & M_4 &= D_{44} M_3 > 0 \\ M_2 &= 4D_{66}\left(D_{11} - D_{66}\right) > 0 & M_5 &= D_{44}^2 M_3 > 0 \quad \Leftrightarrow \quad \delta > 0 \\ M_3 &= 4D_{66}\left[D_{33}\left(D_{11} - D_{66}\right) - D_{13}^2\right] > 0 & M_6 &= D_{66} D_{44}^2 M_3 > 0 \end{aligned} \qquad (4\S1\text{-}6)$$

4§2 - The Backus method.

Backus (1962) introduced a method of homogenization assuming that the equivalent material (in terms of stress and strain) of a bi-layered material is TI (even if the bulk materials are isotropic); then it can be stated that *the homogenized material of a bi-layered material is TI regardless the two layers are TI or not*; that criterion was initially adopted for the analysis of seismic waves but its validity is general and can be extended to the analysis of thin multi-layered materials since foils of bulk materials always exhibit TI features. Without entering into details and assuming the material of each layer isotropic, the stiffness matrix of the homogenized material is given again in terms of five parameters L, M, R, S, T (4§2-1) which are function of $\mu^{(i)}$, $\lambda^{(i)}$, $E^{(i)}$, $\nu^{(i)}$ (Lamè constants, Young, Poisson respectively, $i = 1,2$) and α, the *volume fraction* of the material 1 (that is $\alpha = t^{(1)}/(t^{(1)} + t^{(2)})$ being $t^{(i)}$ the thickness of the material i).

$$L = \left(\frac{\alpha}{\mu^{(1)}} + \frac{1-\alpha}{\mu^{(2)}}\right)^{-1} \quad M = \alpha\mu^{(1)} + (1-\alpha)\mu^{(2)} \quad R = \left(\frac{\alpha}{\lambda^{(1)} + 2\mu^{(1)}} + \frac{1-\alpha}{\lambda^{(2)} + 2\mu^{(2)}}\right)$$

$$S = \alpha\theta^{(1)}\mu^{(1)} + (1-\alpha)\theta^{(2)}\mu^{(2)} \quad T = \alpha\theta^{(1)} + (1-\alpha)\theta^{(2)} \quad \theta^{(i)} = \left(v_S^{(i)}/v_P^{(i)}\right)^2 \qquad (4\S2\text{-}1)$$

$\theta^{(i)}$ is the square of the ratio of the S-wave speed $v_S^{(i)} = [\mu^{(i)}/\rho^{(i)}]^{1/2}$ on the P-wave speed $v_P^{(i)} = [(\lambda^{(i)} + 2\mu^{(i)})/\rho^{(i)}]^{1/2}$ (distortion on dilatation), $\rho^{(i)}$ the density of material i; the constants $D_{11}, D_{13}, D_{33}, D_{44}, D_{66}$ being $D_{12} = D_{11} - 2D_{66}$ are shown in (4§2-2).

$$D_{11} = 4M - 4S + \frac{(1-2T)^2}{R} \quad D_{13} = \frac{1-2T}{R} \quad D_{33} = \frac{1}{R} \quad D_{44} = L \quad D_{66} = M \qquad (4\S2\text{-}2)$$

Thus the parameters L and M give respectively the volume averaged *out-of-plane* and *in-plane* shear modulus of the homogenized material; the other *engineering parameters* can be computed by means of (4§1-3).

4§3 - The strain energy of the TI homogenized material.

The Backus relations can be easily obtained by assuming that the strain energy of the bi-layered material and the homogenized one are the same under two different state of stress, respectively plane and transversal stress.

§ 4.3 i - Plane stress.

The stress-strain relationships of a TI material under plane stress are shown in (4§3-1) and hold both for each of the two materials and the equivalent one (i.e. all are assumed TI); note that (4§3-1) are equal to the isotropic case but ε_z .

$$\begin{cases} \sigma_x = \dfrac{E}{1-\nu^2}\left(\varepsilon_x + \nu\varepsilon_y\right) & \tau_{yz} = 0 \\ \sigma_y = \dfrac{E}{1-\nu^2}\left(\varepsilon_y + \nu\varepsilon_x\right) & \tau_{xz} = 0 \\ \sigma_z = 0 & \tau_{xy} = \mu\gamma_{xy} \end{cases} \quad \begin{cases} \varepsilon_x = \dfrac{1}{E}\left(\sigma_x - \nu\sigma_y\right) & \gamma_{yz} = 0 \\ \varepsilon_y = \dfrac{1}{E}\left(\sigma_y - \nu\sigma_x\right) & \gamma_{xz} = 0 \\ \varepsilon_z = -\dfrac{\nu_z}{E}\left(\sigma_x + \sigma_y\right) & \gamma_{xy} = \tau_{xy}/\mu \end{cases} \tag{4§3-1}$$

Then in the plane stress the equivalent material strain energy is the volume averaged strain energy of the bi-layered material under the same strain field (4§3-2).

$$E_{strain}^{(eq.)} = \alpha E_{strain}^{(1)} + \left(1-\alpha\right) E_{strain}^{(2)}$$
$$\varepsilon_x^{(eq.)} = \varepsilon_x^{(1)} = \varepsilon_x^{(2)} \qquad \varepsilon_y^{(eq.)} = \varepsilon_y^{(1)} = \varepsilon_y^{(2)} \qquad \gamma_{xy}^{(eq.)} = \gamma_{xy}^{(1)} = \gamma_{xy}^{(2)} \tag{4§3-2}$$

It can be easily recognized that in the plane stress the stresses of the equivalent material are the volume averaged stresses of the bi-layered material (4§3-3).

$$\sigma_x^{(eq.)} = \alpha\sigma_x^{(1)} + \left(1-\alpha\right)\sigma_x^{(2)} \qquad \sigma_y^{(eq.)} = \alpha\sigma_y^{(1)} + \left(1-\alpha\right)\sigma_y^{(2)}$$
$$\tau_{xy}^{(eq.)} = \alpha\tau_{xy}^{(1)} + \left(1-\alpha\right)\tau_{xy}^{(2)} \tag{4§3-3}$$

The third of (4§3-3) gives the Backus parameter M in (4§2-1) i.e. the equivalent *in-plane* shear modulus $G^{(eq.)} = \alpha G^{(1)} + \left(1-\alpha\right)G^{(2)}$; rearranging the first two of (4§3-3) the *in-plane* Young modulus $E^{(eq.)}$, the Poisson ratio $\nu^{(eq.)}$ and the shear modulus $\mu^{(eq.)}$ of the equivalent material are straightforward (4§3-4).

$$E^{(eq.)}=\frac{2\beta^{'}\beta^{"}}{\beta^{'}+\beta^{"}} \qquad \nu^{(eq.)}=\frac{\beta^{'}-\beta^{"}}{\beta^{'}+\beta^{"}} \qquad \mu^{(eq.)}=\beta^{"}/2$$
$$\beta^{'}=\alpha\frac{E^{(1)}}{1-\nu^{(1)}}+(1-\alpha)\frac{E^{(2)}}{1-\nu^{(2)}} \quad \beta^{"}=\alpha\frac{E^{(1)}}{1+\nu^{(1)}}+(1-\alpha)\frac{E^{(2)}}{1+\nu^{(2)}} \tag{4§3-4}$$

Note that if, *and only if*, $\nu^{(eq.)}=\nu^{(1)}=\nu^{(2)}$ then $E^{(eq.)}=\alpha E^{(1)}+(1-\alpha)E^{(2)}$ that is <u>*the rule of mixtures holds iff the in-plane Poisson ratios are the same*</u>. Once $E^{(eq.)}$ and $\nu^{(eq.)}$ are computed, the out-of-plane Poisson ratio $\nu_z^{(eq.)}$ is obtained considering that an *in-plane* biaxial stress leads to a volume averaged *out-of-plane* contraction (4§3-5).

$$\varepsilon_z^{(eq.)}=\alpha\varepsilon_z^{(1)}+(1-\alpha)\varepsilon_z^{(2)} \quad \Rightarrow \quad \frac{\nu_z^{(eq.)}}{1-\nu^{(eq.)}}=\alpha\frac{\nu_z^{(1)}}{1-\nu^{(1)}}+(1-\alpha)\frac{\nu_z^{(2)}}{1-\nu^{(2)}} \tag{4§3-5}$$

§ 4.3 ii - Transversal stress.

The relationships of a TI material under transversal stress are shown in (4§3-6).

$$\begin{cases}\sigma_x=\dfrac{\nu_z E E_z}{(1-\nu)E-2\nu_z^2E_z}\varepsilon_z & \tau_{yz}=\mu_z\gamma_{yz}\\ \sigma_y=\dfrac{\nu_z E E_z}{(1-\nu)E-2\nu_z^2E_z}\varepsilon_z & \tau_{xz}=\mu_z\gamma_{xz}\\ \sigma_z=\dfrac{(1-\nu)E E_z}{(1-\nu)E-2\nu_z^2E_z}\varepsilon_z & \tau_{xy}=0\end{cases} \quad \begin{cases}\varepsilon_x=0 & \gamma_{yz}=\tau_{yz}/\mu_z\\ \varepsilon_y=0 & \gamma_{xz}=\tau_{xz}/\mu_z\\ \varepsilon_z=\dfrac{\sigma_z}{E_z}-\dfrac{\nu_z}{E}(\sigma_x+\sigma_y) & \gamma_{xy}=0\end{cases} \tag{4§3-6}$$

Then in the transversal stress the equivalent material strain energy is the volume averaged strain energy of the bi-layered material under the same stress field (4§3-7).

$$E_{strain}^{(eq.)}=\alpha E_{strain}^{(1)}+(1-\alpha)E_{strain}^{(2)}$$
$$\sigma_z^{(eq.)}=\sigma_z^{(1)}=\sigma_z^{(2)} \qquad \tau_{xz}^{(eq.)}=\tau_{xz}^{(1)}=\tau_{xz}^{(2)} \qquad \tau_{yz}^{(eq.)}=\tau_{yz}^{(1)}=\tau_{yz}^{(2)} \tag{4§3-7}$$

It follows that in the transversal stress the strains of the equivalent material are the volume averaged strains of the bi-layered material (4§3-8).

$$\varepsilon_z^{(eq.)}=\alpha\varepsilon_z^{(1)}+(1-\alpha)\varepsilon_z^{(2)} \quad \gamma_{xz}^{(eq.)}=\alpha\gamma_{xz}^{(1)}+(1-\alpha)\gamma_{xz}^{(2)} \quad \gamma_{yz}^{(eq.)}=\alpha\gamma_{yz}^{(1)}+(1-\alpha)\gamma_{yz}^{(2)} \tag{4§3-8}$$

The last two of (4§3-8) give the Backus parameter L in (4§2-1) i.e. the equivalent *out-of-plane* shear modulus $1/G_z^{(eq.)}=\alpha/G_z^{(1)}+(1-\alpha)/G_z^{(2)}$, that is the S-wave modulus D_{44}; rearranging the first of (4§3-8) the *out-of-plane* Young modulus $E_z^{(eq.)}$ (in terms of $\delta^{(eq.)}$) is straightforward (4§3-9).

$$\frac{1}{\left(1-\nu^{(eq.)}\right)E^{(eq.)}}\left(\frac{1}{\delta^{(eq.)}}\right)=\alpha\frac{1}{\left(1-\nu^{(1)}\right)E^{(1)}}\left(\frac{1}{\delta^{(1)}}\right)+\left(1-\alpha\right)\frac{1}{\left(1-\nu^{(2)}\right)E^{(2)}}\left(\frac{1}{\delta^{(2)}}\right)$$

$$1/\mu_z^{(eq.)}=\alpha/\mu_z^{(1)}+\left(1-\alpha\right)/\mu_z^{(2)} \qquad (4\S3\text{-}9)$$

Note that if the two layers are isotropic then $2(1-\nu^{(i)})E^{(i)}\delta^{(i)}=\lambda^{(i)}+2\mu^{(i)}$, $i=1,2$, and (4§3-9) gives the Backus parameter R in (4§2-1), that is the P-wave modulus D_{33}. The relationships (4§3-4), (4§3-5), (4§3-9) give the five *engineering parameters* $E^{(eq.)},\nu^{(eq.)},\nu_z^{(eq.)},E_z^{(eq.)},G_z^{(eq.)}$ by means of elementary calculations; they are in perfect agreement with Backus formulas for isotropic layers in 4§2 - section.

4§4 - Back to real stresses.

For each fiber it is possible to write (4§4-1) (analogous for $\sigma_y{}^{(i)}$, $i=1,2$); note that if, and only if, $\nu^{(eq.)}=\nu^{(1)}=\nu^{(2)}$ then $\sigma_x{}^{(i)}=(E^{(i)}/E^{(eq)})\,\sigma_x{}^{(eq)}$ that is the mismatch of the Poisson ratio always induces a biaxial stress.

$$\sigma_x^{(i)}=\frac{E^{(i)}}{1-\nu^{(i)\,2}}\cdot\frac{1}{E^{(eq)}}\left[\sigma_x^{(eq.)}\left(1-\nu^{(i)}\nu^{(eq)}\right)+\sigma_y^{(eq.)}\left(\nu^{(i)}-\nu^{(eq)}\right)\right] \qquad (i=1,2) \qquad (4\S4\text{-}1)$$

References

[1] ANSYS® Release 10.0A1 UP2006105， Copyright© 1994-2005 by SAS IP as an unpublished work, Rev. ED 8/24/05.

[2] G. Horvay (1956), *Stress Analysis of Perforated Plates*, Report N. 56-RL-1661, General Electric Research Laboratory.

[3] S.P. Timoshenko and J.N. Goodier (1934), *Theory of Elasticity*, Third Edition, McGraw-Hill International Editions.

[4] W.J. O'Donnell and B.F. Langer (1962), *Design of Perforated Plates*, Journal of Engineering for Industry, Trans. ASME, Vol. 84, August 1962.

[5] D.Y.W. Yu and F. Spaepen (2004), *The yield strength on thin copper films on kapton*, Journal of Applied Physics, Vol. 95, No. 6 (15 March 2004), pp. 2991-2997.

[6] A.R. Day et al. (1991), *The elastic moduli of a sheet containing circular holes*, J. Mech. Phys. Solids, Vol. 40, No. 5, pp. 1031-1051.

[7] I. Jasiuk et al. (1994), *Elastic moduli of two dimensional materials with polygonal and elliptical holes*, Appl. Mech. Rev., Vol. 47, No. 1, Part 2, January 1994.

[8] R.S. Kumar et al. (1993), *Elastic Properties of a Polymide Film Determined by Brillouin Scattering and Mechanical Techniques*, Proceedings of 1993 Spring Meeting of the Materials Research Society, San Francisco, April 12-16,1993.

[9] L. Quintieri et al. (2009), *Finite Element Model of the Cylindrical GEM Detector as New Inner Tracker of KLOE2 and Mechanical Characterization of the Employed Materials,* INFN-LNF-09/12(IR) Note, November 11, 2009.

[10] M. Alfonsi et al. (2009), *Activity of CERN and LNF Groups on Large Area GEM Detectors*, Manuscript Number: NIMA_PROCEEDINGS-D-09-00113, Preprint submitted to Elsevier Editorial System™ for NIMA Proceedings.

[11] S.P. Timoshenko, S.W. Krieger (1959), *Theory of Plates and Shells*, Second Edition, McGraw-Hill International Editions.